NASA TECHNICAL MEMORANDUM 107597

DAMAGE DEVELOPMENT IN TITANIUM METAL MATRIX COMPOSITES SUBJECTED TO CYCLIC LOADING
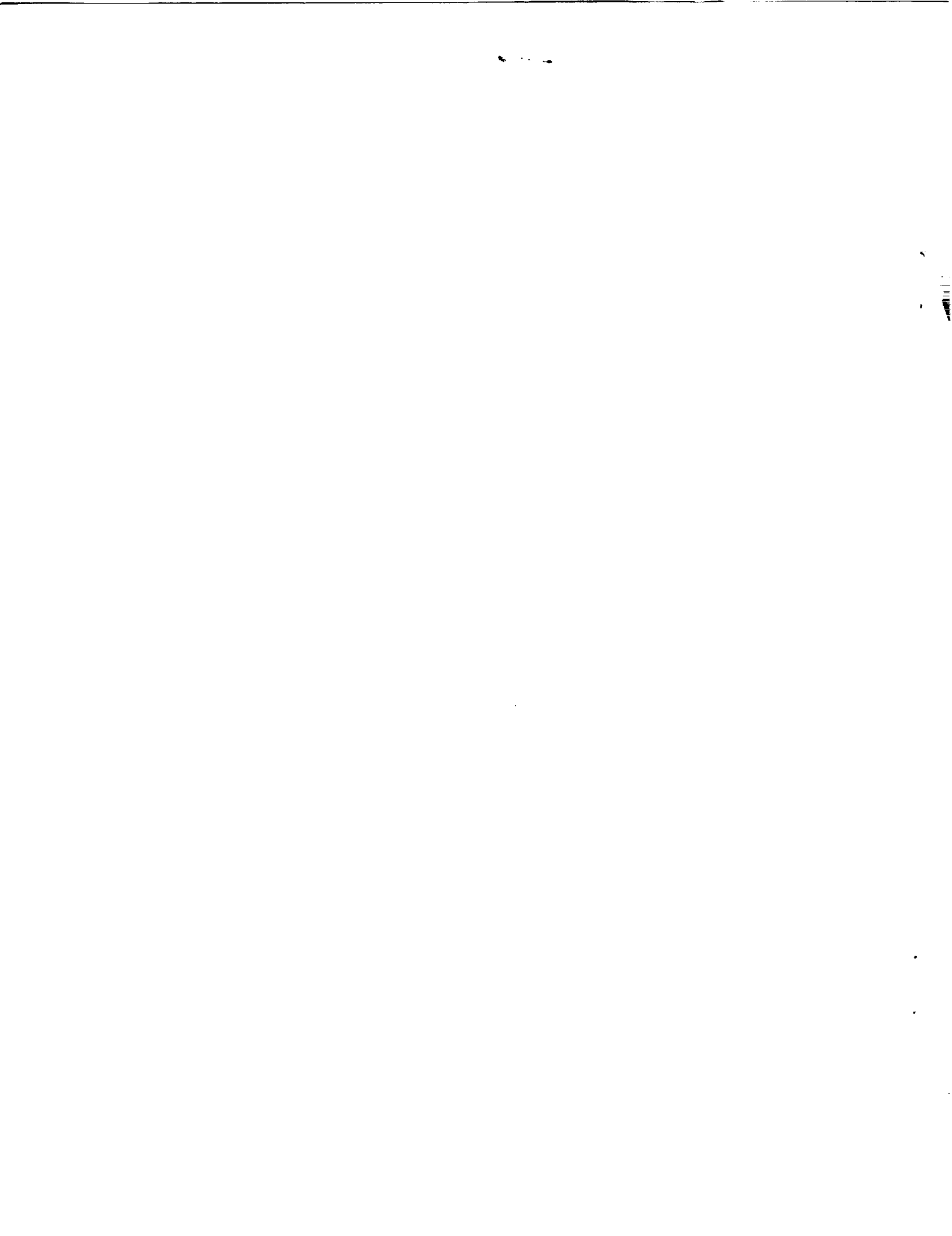
W. S. JOHNSON

April 1992

Presented as a Keynote Lecture at Fatigue and Fracture of Inorganic Composites, Churchill College, Cambridge, UK, March 31-April 2, 1992.

NASA

National Aeronautics and
Space Administration

Langley Research Center
Hampton, Virginia 23665-5225

DAMAGE DEVELOPMENT IN TITANIUM METAL MATRIX COMPOSITES SUBJECTED TO CYCLIC LOADING

*W. S. Johnson**

Abstract: Several lay-ups of SCS-6/Ti-15-3 composites were investigated. Fatigue tests were conducted and analyzed for both notched and unnotched specimens at room and elevated temperatures. Thermo-mechanical fatigue results were also analyzed. Test results indicated that the stress in the 0° fibers is the controlling factor in fatigue life. The static and fatigue strength of these materials is shown to be strongly dependent on the level of residual stresses and the fiber/ matrix interfacial strength. Fatigue tests of notched specimens showed that cracks can initiate and grow many fiber spacings in the matrix material without breaking fibers. Fiber bridging models were applied to characterize the crack growth behavior. The matrix cracks are shown to significantly reduce the residual strength of notched composite. The notched strength of these composites was accurately predicted using a micromechanics-based methodology.

Keywords: interfaces, stiffness loss, finite element analysis, residual strength, effective strain, crack propagation.

INTRODUCTION

Titanium metal matrix composites are currently being considered as structural materials for high temperature applications where weight saving is a premium. Some potential applications of these materials are hypersonic flight vehicles, advanced aircraft engines, missiles, advanced supersonic transports, and advanced fighter aircraft. All of these applications expose the material to repeated mechanical loadings and thermal cycles. In general, the work presented herein is directed toward a material to be used on the structural applications on a hypersonic vehicle. Such a vehicle is expected to have a limited life compared to a typical subsonic aircraft. Therefore, the emphasis for that application is on low-cycle fatigue. Stresses are induced in the composite constituents due to temperature change because of the coefficient of thermal expansion mismatch between the fiber and matrix materials. This, coupled with the different strengths and failure modes of the fiber, matrix and fiber/matrix interface, contributes to a very complex problem in predicting and tracking damage initiation and progression in a

* Senior Research Scientist, NASA Langley Research Center, MS 188E, Hampton, VA 23665-5225, USA

laminated composite. The damage initiation and progression process for a number of different metal matrix composites has been summarized elsewhere[1]. The present paper will show examples of fatigue damage and some of the controlling parameters. In particular, the fatigue behavior of several titanium matrix laminates, notched and unnotched, at room temperature will be discussed. The influence of the fiber/matrix interface strength and the thermal residual stresses on the fatigue damage propagation mode will be illustrated. Thermomechanical fatigue behavior will be modeled and compared with isothermal behavior. This paper is a compilation of previous research on titanium MMC done primarily by the author and his colleagues at the NASA Langley Research Center.

MATERIALS AND TESTING TECHNIQUES

Ti-15-3, a shortened designation for Ti-15V-3Cr-3Al-3Sn, is a metastable beta strip alloy used where cold formability and high strength are desired [2]. In the as-fabricated condition, this titanium has an ultimate strength of 930 MPa, a proportional limit of 690 MPa, and an elastic modulus of 92 GPa [3]. Ti-15-3 is currently under evaluation as a matrix material for high temperature metal matrix composites because it can be economically cold formed into relatively thin sheets while retaining good mechanical properties [2]. The composite laminates were made by hot-pressing Ti-15-3 foils between unidirectional tapes of silicon-carbide fibers. These fibers are designated SCS-6 by Textron Specialty Materials, the producer. The fiber diameter is 0.142 mm and the fiber is assumed to have isotropic properties with a modulus of 400 GPa. Textron Specialty Materials fabricated panels of each of the following lay-ups: $[0]_8$, $[0_2/\pm45]_s$, $[0/90]_{2s}$, $[0/90/0]$ and $[0/\pm45/90]_s$. The fiber volume fractions ranged from 32.5 to 39%, depending on the particular panel. A panel of "fiberless" composite was made identically to the composite but without placing the fiber mats between the foils during fabrication. This resulted in a panel of the matrix material that had seen the same thermal and mechanical history as the matrix in the composite.

The tests were conducted at NASA Langley Research Center, unless otherwise noted, on an 89 kN servohydraulic test stand. For all composite tests load control was used with a loading rate of approximately 0.89 kN/second for the quasi-static tests and a cyclic frequency of 10 Hz for the fatigue tests. Static and fatigue tests of the matrix material were conducted in strain control. Several tests were conducted to determine the rate- and temperature-dependent properties of the matrix material. These tests were conducted under several loading rates and under both strain and load control. For room temperature tests, an extensometer with a 25.4-mm gage length was attached to the edge of the specimens to record strain. For the elevated temperature tests, a water cooled, quartz rod extensometer with a 25.4-mm gage length was used. The specimens were heated using a 5kW induction heater with copper coils. The temperature distribution over the gage length was controlled to within $\pm10^\circ$C.

FIBER/MATRIX SEPARATION

Static and fatigue loading of SCS-6/Ti-15-3 laminates containing off-axis plies resulted in a knee in the stress-strain curve well below the stress level anticipated for the onset of matrix plasticity [3]. Figure 1 shows the cyclic stress-strain response of a $[90]_8$ laminate. The knee in the first cycle, Figure 1(a) occurred at approximately 155 MPa, well below the matrix material's minimum proportional limit of 690 MPa. The unloading elastic modulus was also less than the initial elastic modulus, thus indicating that some sort of damage had occurred in the laminate. After the first few cycles, the stress-strain response was identical for all subsequent cycles until just before failure. Figure 1(b) shows a typical curve for the 11th cycle. Here, the unloading curve closely follows the loading curve. This behavior indicates an opening and closing phenomenon which was found to be due to separation of the fiber/matrix interface in the off-axis plies. The applied mechanical loading causes the fiber and matrix in the off-axis plies to separate once the thermally induced compressive radial residual stresses around the fiber have been overcome. This was confirmed using the edge replica technique [1,3]. An example of an edge replica indicating the fiber/matrix separation around a 90° fiber of an $[0/90]_{2s}$ laminate is shown in Figure 2. Reference 3 discusses the fiber/matrix interface separation that occurred in these composites in detail.

Johnson, Lubowinski, and Highsmith[3] suggested that thermal residual stresses were responsible for the opening and closing behavior observed in the composite. These laminates are consolidated at such a high temperature that the matrix and fiber are initially stress free. However, as the composite cools, internal stresses are developed in the constituents due to the difference in the coefficients of thermal expansion of the fiber and the matrix. A simple concentric cylinder model was used to estimate the thermal residual stresses. For the silicon-carbide/titanium system, coefficients of thermal expansion of 4.86×10^{-6} cm/cm/°C and 9.72×10^{-6} cm/cm/°C [2] were used for the fiber and matrix, respectively. It was assumed that any stresses that developed during the fabrication process at absolute temperatures greater than one half of the melting point of the matrix would be relieved due to stress relaxation [4]. Therefore, a temperature change of 555°C was used. For the as-fabricated unidirectional lamina at room temperature, the analysis predicted the following stresses in the matrix material near the fiber/matrix interface: radial stress, -138 MPa; tangential stress, 276 MPa; and axial (fiber-direction) stress, 207 MPa. The compressive radial and tensile tangential (hoop) stresses cause the matrix to close around the fiber upon unloading. Even when the fiber/matrix interface has failed, these residual stresses must be overcome before the fiber and matrix will separate. For those specimens tested at temperatures approaching 555°C and greater, the residual thermal stresses were considered to be insignificant so that the fiber/matrix interfaces in the off-axis plies would separate immediately upon loading once the interface had failed.

FATIGUE OF UNNOTCHED SPECIMENS

Fatigue at Room Temperature

S-N data was experimentally determined at room temperature (RT) for four different lay-ups containing 0° plies as shown in Figure 3 [3]. The stress-strain response was monitored during the fatigue life. Laminates containing off-axis plies lost stiffness very early in the cycling history due to the fiber/matrix interface separations. After a few cycles, the stiffness stabilized and the cyclic strain range was recorded. This stabilized strain range was multiplied by the fiber modulus (400 GPa) to determine the cyclic stress range in the fiber. A plot of the 0° fiber cyclic stress range against life for the different laminates is shown in Figure 4. The fatigue data from the four different laminates were correlated very well by the 0° fiber stress range. The applied stress ratio was 0.1. Since there is a small compressive residual stress introduced into the fiber during the thermal cycle in the fabrication process that is lay-up dependent, the stress ratio in the 0° fiber is slightly different for each lay-up and each applied stress level. The stress range in the fiber varied between approximately 0.0 and 0.1. Since the laminate will not fail until the 0° fiber fails, it is reasonable to assume that the stress in the 0° fiber will dictate fatigue life. The measured stabilized strain range is also plotted against the number of cycles to failure in Figure 4.

Also plotted in Figure 4 is the strain-controlled fatigue life of the Ti-15-3 matrix material (i.e., the "fiberless" composite). Comparing the fatigue life in terms of the strain range of the 0° fibers to the matrix data up to 60,000 cycles, it appears that for the same cyclic strain range the fibers would fail first. This was confirmed by examining failure surfaces of fatigued laminates. There was no evidence of significant matrix cracking except in one $[0]_8$ specimen that was cycled at an applied laminate stress of 690 MPa and broke at 516,000 cycles [3]. This test is shown as the run-out data point in Figures 3 and 4. This specimen had such a long life that the matrix curve may well have intersected the fiber failure curve. Thus, knowledge of the fatigue behavior of the constituents is useful for the prediction and interpretation of the composite fatigue response. The constituent fatigue behavior will provide insight into whether the matrix or the fiber will be the first to fail for a given applied cyclic stress. This is especially true for 0° laminates that are not complicated by interfacial failure in the off-axis plies.

Fatigue at High Temperature

Unnotched fatigue tests were conducted at 650^oC on the SCS-6/Ti-15-3 laminates described above and the results are reported in detail by Pollock and Johnson [5]. The cyclic stress range in the 0° fibers versus number of cycles to failure is plotted with the room temperature data in Figure 5. The elevated temperature data is more scattered than the room temperature data. At this elevated temperature the matrix could creep during cycling and creep ratcheting (an accumulation of strain) would result. As the strain accumulates, the maximum stress in the fiber increases. The laminates with off-axis plies would be expected to creep more than the $[0]_8$ laminate, thus the cyclic R ratio of

the fiber stress will be higher for the $[0/\pm45/90]_s$ and $[0/90]_{2s}$ laminates. This may, in part, explain why the $[0/\pm45/90]_s$ and $[0/90]_{2s}$ laminate results fall below the $[0]_8$ laminate results in Figure 5 when based only on the measured 0° fiber stress range.

Figure 6 compares the maximum strain versus cycles to failure of a unidirectional composite to the maximum strain versus cycles to failure of the matrix loaded in strain control [5]. The fatigue test of the unidirectional specimen was considered to be an in-situ fatigue test of the fibers. For high maximum strains (short lives) the initial damage developed in the fibers and the composite had a shorter life than the matrix alone. For low maximum strains (long lives) the initial damage developed in the matrix and the matrix had a shorter life than the composite. Where the two curves intersect, both the matrix and the fibers were equally likely to develop fatigue damage. Figure 7 shows three polished surfaces taken at locations away from the specimen fracture surface for unidirectional specimens with short, medium and long lives. The high stress, short life specimen exhibits many fiber breaks but no significant matrix cracking (the lines visible in the matrix are grain boundaries). The medium life specimen has both fiber breaks and some short matrix cracks. The low stress, long life specimen exhibits no fiber breaks but several long matrix cracks. Therefore, it is reasonable to use the fatigue response of the matrix material and the in-situ 0° fiber to predict at which strain levels the fiber will fail before matrix cracking and at which strain levels matrix cracking will precede fiber failure.

Thermomechanical Fatigue

Both thermal and mechanical stresses are developed in the constituents of a laminate during thermomechanical fatigue (TMF). Since constituent stresses are not necessarily related to the measurable laminate strains, an analysis is needed to calculate the constituent and laminate behavior of arbitrary lay-ups subjected to arbitrary combinations of mechanical and thermal loading. The *VISCOPLY* code is a micromechanics analysis[6] based on constituent properties developed by NASA Langley. The program uses the vanishing fiber diameter (VFD) constitutive model [7] to calculate the orthotropic properties of the plies. These ply properties are then used in a laminated plate analysis to predict overall laminate response. Both the fiber and the matrix can be modeled as a thermo-viscoplastic material. Combinations of thermal and mechanical loads can be modeled. Sequential jobs can be run for various load and temperature profiles. Fiber and matrix average stresses and strains in each ply and the overall composite response under thermomechanical loading conditions are calculated. The *VISCOPLY* program, due to the nature of the VFD model, does not account for local stress concentrations around the fiber nor for lateral constraint in a ply due to the presence of the fiber. However, based upon the author's experience using the VFD model for over 12 years on numerous MMC's, the model predicts general laminate response very well, usually within 10 percent of measured response.

The *VISCOPLY* program was used to predict the laminate response of unidirectional SCS-6/Ti-15-3 composites [6]. Neat Ti-15-3 matrix material was tested to determine the

required thermo-viscoplastic material constants. An example of these predictions is shown in Figure 8 for an in-phase TMF test conducted at NASA Lewis Research Center. The prediction captures the essence of the loading-unloading behavior of the composite. The fatigue behavior as a function of maximum applied stress for in-phase and out-of-phase TMF is shown in Figure 9. The in-phase loadings resulted in earlier failures but the specimens lost very little stiffness prior to failure. On the other hand, the out-of-phase loadings resulted in significant stiffness loss due to matrix cracking prior to failure. The *VISCOPLY* program was used to predict the fiber and matrix stresses during an in-phase and an out-of-phase TMF cycle between 93-538°C and 45-896 MPa as shown in Figure 10. The fiber stresses are highest for the in-phase test, explaining the earlier laminate fatigue failures. However, the matrix stresses are higher for the out-of-phase loadings, thus explaining the earlier matrix cracking and the resulting stiffness loss measured during the out-of-phase loadings[8]. When each test shown in Figure 9 was analyzed and the 0^0 fiber stress range was plotted versus the number of cycles to failure, the in-phase and out-of-phase data collasped into a narrow band as shown in Figure 11.

Other TMF and isothermal data were analyzed and are plotted in Figure 12 [6]. Within a given test condition, i.e., temperature, loading frequency, time at temperature, etc., the 0^0 fiber stress range seems to correlate with the number of cycles to failure. However, as the test conditions change the fatigue behavior of the fiber appears to change. Since the plot is of stress range in the fiber, the increased loading of the fiber due to matrix stress relaxation is not accounted for. Higher temperatures and slower cycling would both contribute to more load being shifted to the fiber from the matrix. Additional time at temperature could also cause additional fiber/matrix interface reactions that could effect the mechanical behavior [9,10].

Effect of Interface Strength and Residual Stresses on Fatigue

Naik, Johnson, and Pollock [10] investigated the effect of a high temperature cycle (1010°C) used to simulate a superplastic forming/diffusion bonding (SPF/DB) fabrication cycle on the mechanical properties of a [0/90/0] lay-up of SCS-6/Ti-15-3. The high temperature cycle (SPF/DB) increased the strength and stiffness of the matrix material, had little or no effect on the fiber properties but significantly reduced the static and fatigue strength of the laminate as shown in Figure 13. The fracture surfaces in Figure 13 showed a change in the failure mode due to the SPF/DB cycle. In the as-fabricated (ASF) specimen the fiber/matrix interface was weaker and the thermal residual stresses were less compressive than in the SPF/DB specimen; thus, the damage tended to grow around the fibers, debonding the fiber/matrix interface. This produced a tortuous crack path in the matrix and extensive fiber pull-out. In the SPF/DB specimen the residual stresses were sufficiently high and the fiber/matrix interface strong enough to cause the matrix cracks to grow through the fiber resulting in a planar failure surface with little or no fiber pull-out. A shear-lag analysis indicated that the latter failure mode produced a greater stress concentration in the first fiber ahead of the crack, thus explaining the reduction in strength of the SPF/DB specimen.

These results [10] indicate that for a high strength matrix material, such as a titanium alloy, one can make the fiber/matrix interface too strong, thus, sacrificing laminate strength by changing the mode of failure. Conversely, if the interface is too weak, the required load transfer between fiber and matrix necessary for optimum moduli and shear properties will not occur.

FATIGUE OF NOTCHED SPECIMENS

Fatigue behavior near local stress concentrations can be complex. The initiation process at a notch may be very different from the subsequent damage growth process. Depending upon the design philosophy adopted, one process may be more important than the other; however, both damage initiation and growth need to be understood.

Fatigue Crack Initiation

Naik and Johnson[11] experimentally generated cycles to crack initiation versus applied loading for several different lay-ups and notch geometries. They observed that cracks initiated in the matrix material and grew without breaking fibers. To explain the matrix crack initiation process, Hillberry and Johnson [12] developed the strain controlled matrix fatigue data shown previously in Figure 4. The matrix fatigue data was replotted in terms of the Smith-Watson-Topper effective strain parameter, $\Delta\varepsilon_{eff}$ [13] as shown in Figure 14. Hillberry and Johnson [12] modified the Smith-Watson-Topper effective strain parameter to predict cycles to fatigue damage initiation in the matrix material next to a notch. The modification includes the calculated thermal residual stresses in the matrix, σ^r, and the orthotropic stress concentration factor, K_t, as follows

$$\Delta\varepsilon_{eff} = [(K_t\varepsilon_{max} + \sigma^r/E_m) K_t(\Delta\varepsilon/2)]^{1/2}$$

where E_m is the matrix modulus, ε_{max} is the maximum applied strain to the specimen, and $\Delta\varepsilon$ is the applied strain range.

For each experimental test, the effective strain parameter was calculated using the above equation and plotted versus the number of cycles to observed crack initiation. The results are shown in Figure 15. Very good agreement was found between the experiments and predictions based on the matrix fatigue data alone.

The residual stress in the matrix is an important contributor to the total effective strain. At a lower values of $\Delta\varepsilon_{eff}$ in Figure 15, e.g., 0.0035, σ^r/E is 35 percent of the $(K_t \varepsilon_{max} + \sigma^r/E)$ term. Without the residual stress term the effective strain parameter would be reduced by 59 percent. At a higher values of $\Delta\varepsilon_{eff}$ in Figure 15, e.g., 0.0065, the effective strain parameter would be reduced by 46 percent since the σ^r/E is 21 percent of the $(K_t \varepsilon_{max} + \sigma^r/E)$ term. Obviously if the composite data points were shifted down by these percentages, the effective strain parameter would not correlate the data. This illustrates the importance of including the residual stress term in the modified effective strain parameter.

Fatigue Crack Growth from Notches

Fatigue cracks were observed in notched $[0]_8$, $[0/90]_{2s}$, and $[0/90/0]$ laminates at cyclic stress levels above those required for crack initiation but well below the laminate net section static strength [11]. The specimens were periodically radiographed during the tests to monitor fiber breaks. After the tests (but prior to specimen failure), the specimen surfaces were either polished or acid etched to reveal the matrix cracks and fibers in the surface ply. Multiple matrix cracks had initiated at and grown from the notches. Harmon and Saff [14] reported similar results for unidirectional SCS-6/Ti-15-3 center hole specimen. Figure 16 shows a typical matrix crack growing from the edge of a hole in a $[0/90]_{2s}$ specimen. The polished surface clearly shows that the matrix crack grew around and past the fibers. Also, a long debond between the fiber next to the hole and the matrix on the side toward the hole was seen. This type of debonding can significantly reduce the stress concentration at the edge of the notch. One can nominally predict the stress level at which the fibers next to the notch should fail based on the applied loading and calculated stress concentration for the undamaged state. However, because of damage such as shown in Figure 16, the stress concentration may be reduced so that only the matrix would fail and not the fibers.

Bigelow and Naik[15] developed a macro-micromechanics finite element approach to calculate the local stresses around a continuous fiber at a global stress discontinuity, such as a notch tip. This approach was used by Bigelow and Johnson[16] to predict the notch-tip interface stresses in the matrix material (Figure 17) due to a remote stress of 1 MPa on a double edge notched $[0/90]_{2s}$ SCS-6/Ti-15-3 specimen with the same geometry as the specimen described above. $\theta = 180°$ is the side of the $0°$ fiber toward the notch tip. In this direction, the radial stresses are highly tensile; thus, the matrix would tend to pull away from the fiber. In fact, the radial stress value next to the notch tip is approximately 450% of the remotely applied loading. Assuming linear-elastic behavior, a remote load of 31 MPa would be required to overcome the radial component of the thermal residual stresses calculated earlier (-138 MPa) and fail the fiber/matrix interface if the interface strength is low as it has been shown to be [3]. This type of analysis can give good insight into the cause of fiber/matrix interface failure such as shown in Figure 16. The axial stress is high due to the local stress concentration. Once the notch-tip $0°$ fiber/matrix interface debonds, the stress concentration will decrease by approximately one third [16].

Prediction of Growth Rates in Bridged Cracks

Bakuckas and Johnson [17] conducted an analytical and experimental investigation of the effect of fiber bridging on crack growth in $[0]_8$ SCS-6/Ti-15-3. The specimens tested contained center slits with initial notch-length-to-width-ratios of 0.30 and 0.35. Under constant amplitude loading the crack growth rate decreased as the crack length increased. The fiber bridging reduced the crack driving force as the crack grew. Since the crack in the composite is growing only in the matrix material, the crack growth rate in the composite should correlate with the crack growth rate in the matrix material

alone if the correct crack driving force in the matrix, ΔK_{mat}, is defined. Figure 18 shows crack growth rate versus ΔK data for the Ti-15-3 material. The figure also shows the composite data plotted with ΔK_{app}, the crack driving force calculated without accounting for the fiber bridging. The ΔK_{app} does not collapse the composite crack growth data to the Ti-15-3 data. The effect of the fibers bridging the matrix crack must be incorporated into the definition of ΔK_{mat}.

Several fiber bridging models which combine a continuum fracture mechanics analysis and a micromechanics analysis were investigated [18-20]. In all of these models, the intact fibers in the wake of the matrix crack are modeled using a continuous closure pressure. Fiber/matrix debonding occurs as the crack progresses past each fiber. An unknown constant shear stress τ is assumed to act on the debonded fiber/matrix interface. The model proposed by McMeeking[20] provided the most accurate predictions of the measured fiber/matrix debond length and crack opening displacements for test data available, as well as collapsing the da/dN data as shown in Figure 18. The values of τ used to fit the data are also shown in Figure 18.

Effect of Matrix Cracking on Residual Strength

Matrix cracks initiate and grow from notches at cyclic stress levels of less than one third of the ultimate strength of notched virgin specimen. In cases where only matrix cracks occur with no accompanying fiber failures, one needs to be able to assess the effect of this damage on residual strength. Bakuckas, Johnson, and Bigelow[21] conducted an experimental and analytical study of $[0/90]_{2s}$ laminate containing a center hole specimen with a hole diameter to specimen width ratio of 0.33. The residual strengths were experimentally determined for a virgin specimen and for a specimen that was saturated with matrix cracks after being subjected to cyclic loading between 25 and 250 MPa for 200,000 cycles. The residual strengths were 525 MPa and 325 MPa, respectively. The matrix cracks resulted in a strength reduction of 38%. Thus, the effect of the matrix cracks is significant.

The three dimensional finite element program *PAFAC* [22] was used to determine the effects of the matrix cracks on the stress concentration in the 0° fibers and to predict the residual strengths of both the virgin and post-fatigued specimens. For the virgin condition the composite was initially modeled with the undamaged properties of the matrix and fiber and assuming a perfect fiber/matrix interface. As the virgin specimen was analytically loaded, the fiber/matrix interfaces were assumed to fail in the 90° plies, as previously discussed. For the post-fatigued test the modulus of the matrix was reduced by 69% to account for the saturated state of the matrix cracks. The modulus reduction was determined by calculating the required matrix modulus to account for the stiffness loss in the unnotched crack-saturated portion of the specimen. A schematic of the observed cracking pattern and the finite element model are shown in Figure 19. Notice that the portion just above and below the hole did not develop matrix cracking and was modeled appropriately. The fiber strength was determined from unnotched coupons by recording the strain to failure and multiplying it by the

fiber modulus. The predicted and measured residual strengths are shown in Figure 20. The point at which the predicted notch tip 0° fiber stress crosses the fiber strength line represents the predicted laminate failure. The $[0/90]_{2s}$ laminate failure was observed to be catastrophic, i.e., when the first fiber failed, the specimen failed. Using this micromechanics-based strength prediction methodology for the notched laminate resulted in excellent predictions.

SUMMARY

This paper summarizes research conducted by the author and his colleagues on notched and unnotched fatigue of composite laminates made of a titanium alloy matrix reinforced with silicon-carbide fibers (SCS-6/Ti-15-3). In the unnotched laminates, damage starts as fiber/matrix interface failures in the off-axis plies. This results in a stiffness loss early in the fatigue life. These failed interfaces in the off-axis plies result in a bilinear stress-strain response for the laminate. This could present potential design problems.

The fatigue life of the unnotched laminates tested under the same temperature, cyclic frequencies and time at temperatures conditions was shown to be a function of the stress range in the 0° fibers for isothermal, nonisothermal, and thermomechanical fatigue conditions. However, the 0° fiber stress range-cycles to failure relationship did vary for different temperature and time at temperature conditions, indicating a fiber/matrix reaction effect or an accumulative strain effect at elevated temperatures.

A laminate analysis, *VISCOPLY*, was used to account for mechanical, thermal, and rate dependent behavior based on constituent material properties. The analysis calculates fiber and matrix stresses and strains in each ply of any arbitrary symmetric laminate. The analysis was successfully used to predict laminate response under thermomechanical fatigue loading. An analysis such as *VISCOPLY* is required to calculate consituent stresses since such stresses cannot be measured directly under thermomechanical fatigue conditions.

The strength of the interface and the magnitude of the thermal residual stresses were shown to play a significant role in the laminate failure process. High interface strengths and high residual stresses can reduce the laminate static and fatigue strength.

Fatigue damage initiation at notches was predicted using unnotched matrix data and an effective strain parameter that accounted for orthotropic stress concentration and residual thermal stresses in the matrix. Good correlation between the predicted and experimental results were obtained for several different lay-ups for both center hole and edge notched specimens. Matrix fatigue cracks were found to grow long distances in the laminate without breaking the 0° fibers in the crack path. Fiber/matrix interface debonding early in the fatigue life resulted in a significant reduction in the stress concentration in 0° fibers at a notch tip. The calculated stress concentrations for virgin notched specimens can be used to calculate damage initiation in a virgin specimen but they do not apply to damage propagation or fracture in the specimen after damage has initiated.

Several fiber bridging models were applied to experimental data obtained from unidirectional laminates containing center slits. Fiber bridging models were shown to collapse the composite crack growth data onto a matrix only crack growth rate curve by using the constant shear stress due to fiber/matrix debonding as a fitting parameter.

Matrix cracking around notches occurred at low cyclic stress levels. Since these matrix cracks were generated at low stress levels and did not break fibers, one might believe that this damage is largely cosmetic, but, in fact, the residual strength was significantly reduced, making these matrix cracks a serious consideration. The effect of these matrix cracks on residual strength was accurately modeled by a micromechanics based strength prediction methodology, using a three dimensional finite element program.

In conclusion, the subject research has established a good fundamental understanding of fatigue damage initiation and propagation in continuous fiber reinforced titanium matrix composites at both room and elevated temperatures. The causes of initial damage on both the global and local levels are becoming well defined. Seemingly insignificant factors, such as thermal residual stresses and interfacial strengths, play profound roles in almost every aspect of the fatigue life, from initiation to fracture, and, thus, they must not be overlooked.

ACKNOWLEDGMENT

REFERENCES

(1) Johnson, W. S., "Fatigue Testing and Damage Development in Continuous Fiber Reinforced Metal Matrix Composites", *Metal Matrix Composites: Testing, Analysis and Failure Modes*, ASTM STP 1032, W. S. Johnson, Ed., Philadelphia, PA, 1989, pp. 194-221.

(2) Rosenberg, H. W., *Journal of Metals*, Vol. 35, No. 11, Nov 1986, pp. 30-34.

(3) Johnson, W. S., Lubowinski, S. J., and Highsmith, A. L., "Mechanical Characterization of SCS-6/Ti-15-3 Metal Matrix Composites at Room Temperature," *Thermal and Mechanical Behavior of Ceramic and Metal Matrix Composites*, ASTM STP 1080, J. M. Kennedy, H. H. Moeller, and W. S. Johnson, Eds. Philadelphia, 1990, pp. 193-218.

(4) Dieter, G. E., *Mechanical Metallurgy*, 2nd ed., McGraw-Hill, New York, 1976, pp. 451-489.

(5) Pollock, W. D. and Johnson, W. S., "Characterization of Unnotched SCS-6/Ti-15-3 Metal Matrix Composites at 650°C," *Composite Materials: Testing and Design (Tenth Volume)*, ASTM STP 1120, Glenn Grimes, Ed., Philadelphia, 1992, pp. 175-191.

(6) Mirdamadi, M., Johnson, W. S., Bahei-El-Din, Y. A., and Castelli, M. G., Analysis of Thermomechanical Fatigue of Unidirectional Titanium Metal Matrix Composites, NASA TM 104105, July 1991, 33 pgs.

(7) Bahei-El-Din, Y. A., "Plasticity Analysis of Fibrous Composite Laminates Under Thermomechanical Loads," *Thermal and Mechanical Behavior of Ceramic and Metal Matrix Composites*, ASTM STP 1080, J. M. Kennedy, H. H. Moeller, and W. S. Johnson, Eds. Philadelphia, 1990, pp. 20-39.

(8) Castelli, M. G., Bartolotta, P. A., and Ellis, J. R., "Thermomechanical Fatigue Testing of High Temperature Composites: Thermomechanical Fatigue (TMF) Behavior of SiC(SCS-6)/Ti-15-3," *Composite Materials: Testing and Design (Tenth Volume)*, ASTM STP 1120, Glenn Grimes, Ed.,Philadelphia, 1992, pp. 70-86.

(9) Jeng, S. M., Yang, C. J., Alassoeur, P, and Yang, J.-M., "Deformation and Fracture Mechanisms of Fiber-Reinforced Titanium Alloy Matrix Composite," *Composites Design, Manufacture, and Application*, Paper 25-C, ICCM/VIII, S. W. Tsai and G. S. Springer, Eds., 1991.

(10) Naik, R. A., Johnson, W. S., and Pollock, W. D., "Effect of a High Temperature Cycle on the Mechanical Properties of Silicon Carbide/Titanium Metal Matrix Composite," *Journal of Material Science*, Vol. 26, 1991, pp. 2913-2920.

(11) Naik, R. A., Johnson, W. S., "Observations of Fatigue Crack Initiation and Damage Growth in Notched Titanium Matrix Composites", *Composite Materials: Fatigue and Fracture (Third Volume)*, ASTM STP 1110, T. K. O'Brien, Ed., Philadelphia, 1991, pp. 753-771.

(12) Hillberry, B. M. and Johnson, W. S., "Prediction of Matrix Fatigue Crack Initiation in Notched SCS-6/Ti-15-3 Metal Matrix Composites," to appear in *Journal of Composites Technology and Research*, ASTM, Fall 1992.

(13) Smith, K. N., Watson, P., and Topper, T. H., "A Stress-Strain Function for Fatigue of Metals," *Journal of Metals*, Vol. 5, No. 4, Dec. 1970, pp. 767-778.

14) Harmon, D. M., and Saff, C. R., "Damage Initiation and Growth in Fiber Reinforced Metal Matrix Composites," *Metal Matrix Composites: Testing, Analysis and Failure Modes*, ASTM STP 1032, W. S. Johnson, Ed., Philadelphia, PA, 1989, pp. 237-250.

(15) Bigelow, C. A., and Naik, R. A., "A Macro-Micromechanics Analysis of a Notched Metal Matrix Composite," *Composite Materials: Testing and Design (Tenth Volume)*, ASTM STP 1120, Glenn Grimes, Ed., Philadelphia, 1992, pp. 222-233.

(16) Bigelow, C. A. and Johnson, W. S., "Effect of Fiber-Matrix Debonding on Notched Strength of Titanium Metal Matrix Composites," NASA TM-104131, National Aeronautics and Space Administration, Washington, DC., Aug. 1991, 32 pgs.

(17) Bakuckas, J. G., Jr., and Johnson, W. S., "Application of Crack Bridging Models to Fatigue Crack Growth in Titanium Matrix Composites," NASA TM 107588, National Aeronautics and Space Administration, Washington, DC., April 1992.

(18) Marshall, D. B., Cox, B. N., and Evans, A. G., "The Mechanics of Matrix Cracking in Brittle-Matrix Fiber Composites," *Acta Metall.*, Vol. 33, No. 11, 1985, pp. 2013-2021.

(19) McCartney, L. N., "Mechanics of Matrix Cracking in Brittle-Matrix Fibre-Reinforced Composites," *Proc. R. Soc. Lond.*, A 409, 1987, pp. 329-350.

(20) McMeeking, R. M., and Evans, A. G., "Matrix Fatigue Cracking in Fiber Composites," *Mechanics of Materials*, Vol. 9, 1990, pp. 217-227.

(21) Bakuckas, J. G., Jr., Johnson, W. S., and Bigelow, C. A., "Fatigue Damage In Cross-Ply Titanium Metal Matrix Composites Containing Center Holes," NASA TM-104197, National Aeronautics and Space Administration, Washington, DC., January 1992, 30 pgs.

(22) Bigelow, C. A., and Bahei-El-Din, Y. A., Plastic and Failure Analysis of Composites (PAFAC). LAR-13183, COSMIC, University of Georgia, 1983.

SCS-6/Ti-15-3
[90]₈

(a) 1st loading cycle

(b) 11th loading cycle
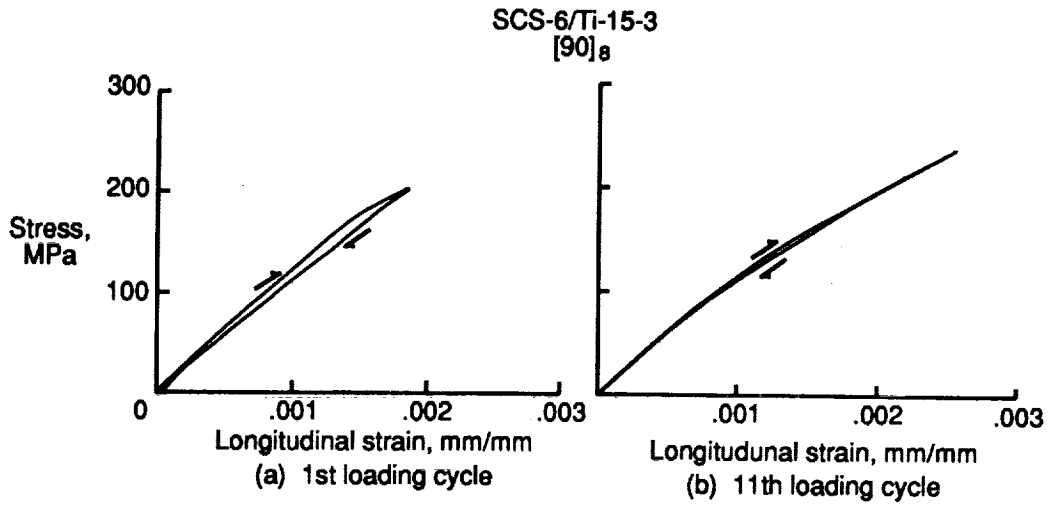
Figure 1. Stress-strain response showing nonlinearity due to fiber/matrix separation[3].
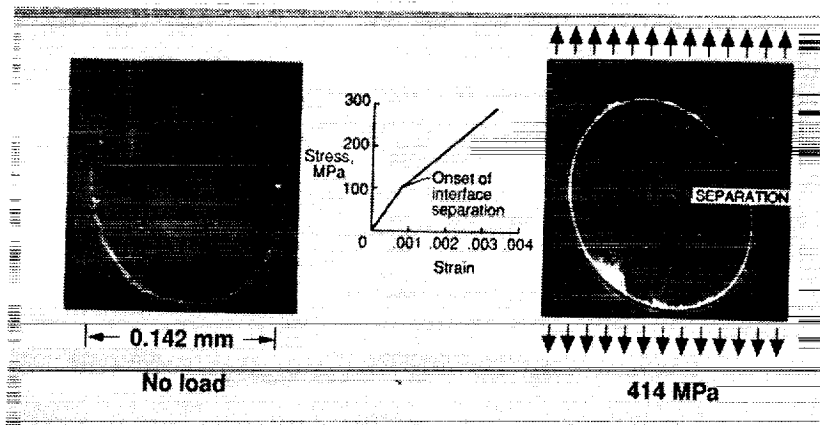

Figure 2 Fiber/matrix interface failure around a 90° fiber in an SCS₆/Ti-15-3 [0/90]₂ₛ composite[3].
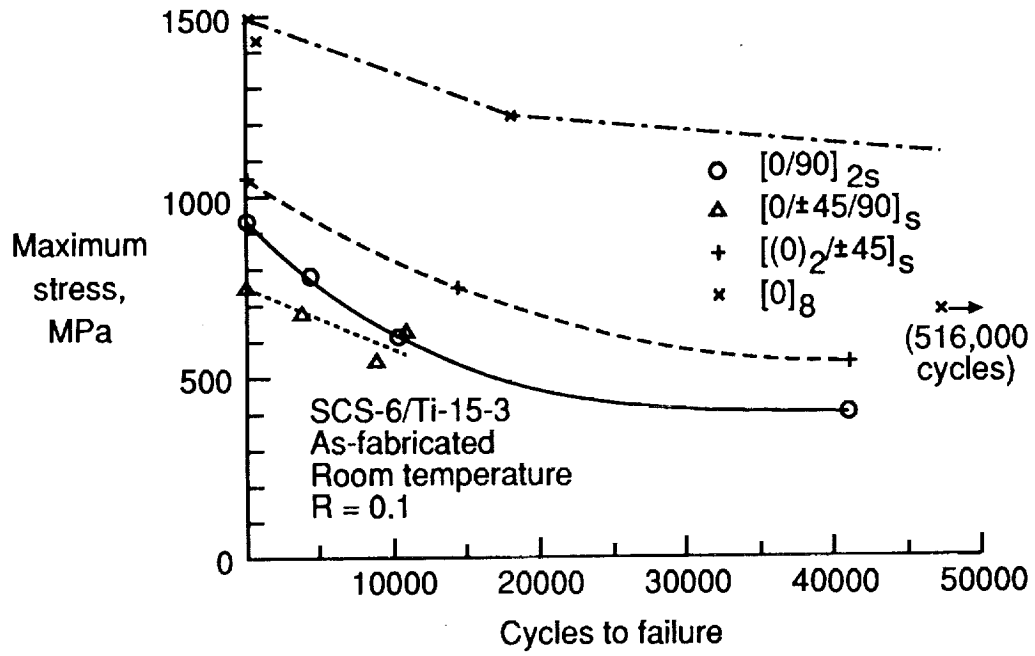
14

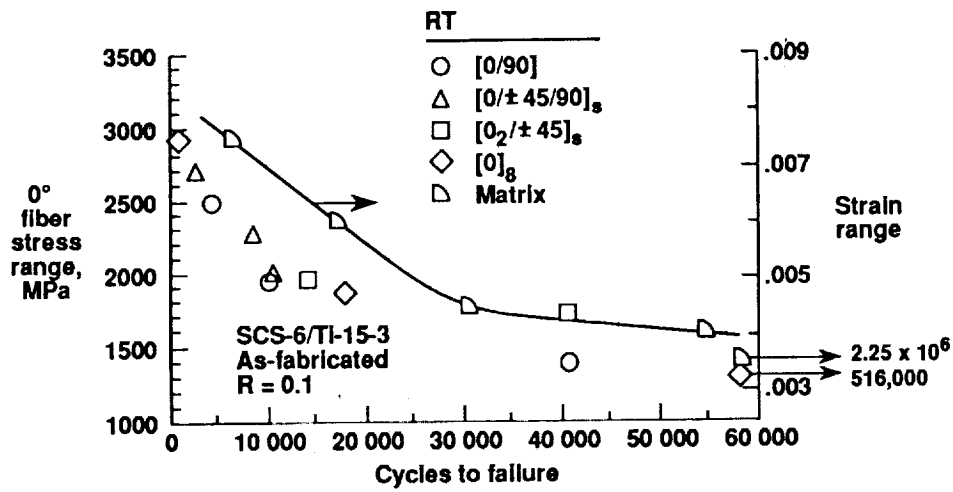Figure 3. S-N curves for SCS-6/Ti-15-3 laminates containing 0° plies[3].

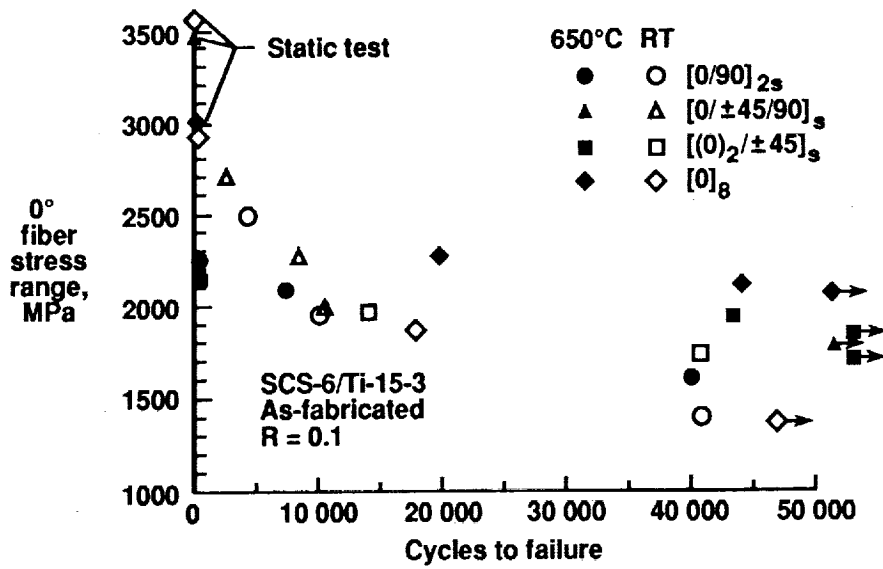Figure 4. Cyclic stress range in 0° fiber versus number of cycles to laminate failure[3]. Matrix fatigue life is shown in terms of strain range.

Figure 5. 0° fiber stress range versus number of cycles to failure at 650°C and RT[5].
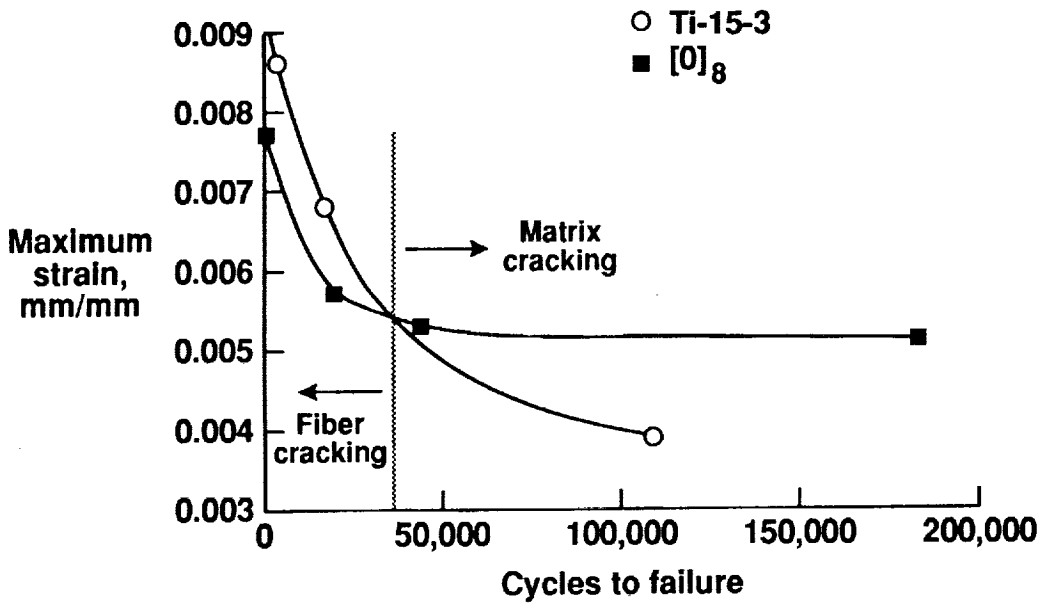
Figure 6. The life of the unidirectional composite and the matrix as a function of maximum strain at 650°C [5].

16
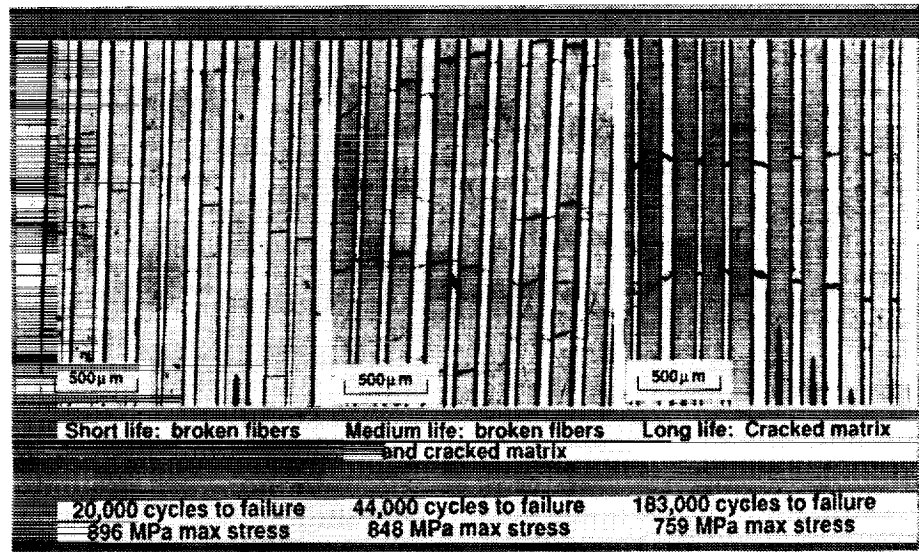
Figure 7. Sections parallel to the loading axis in unidirectional coupons behind the failed surface [5].
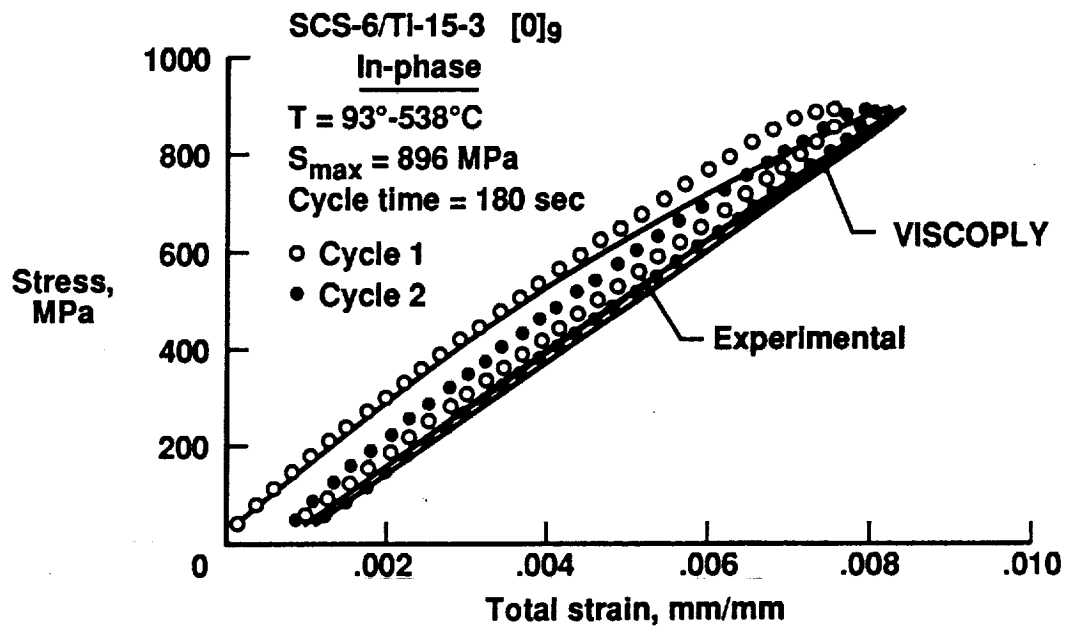
Figure 8. Prediction of composite response under in-phase TMF [6].
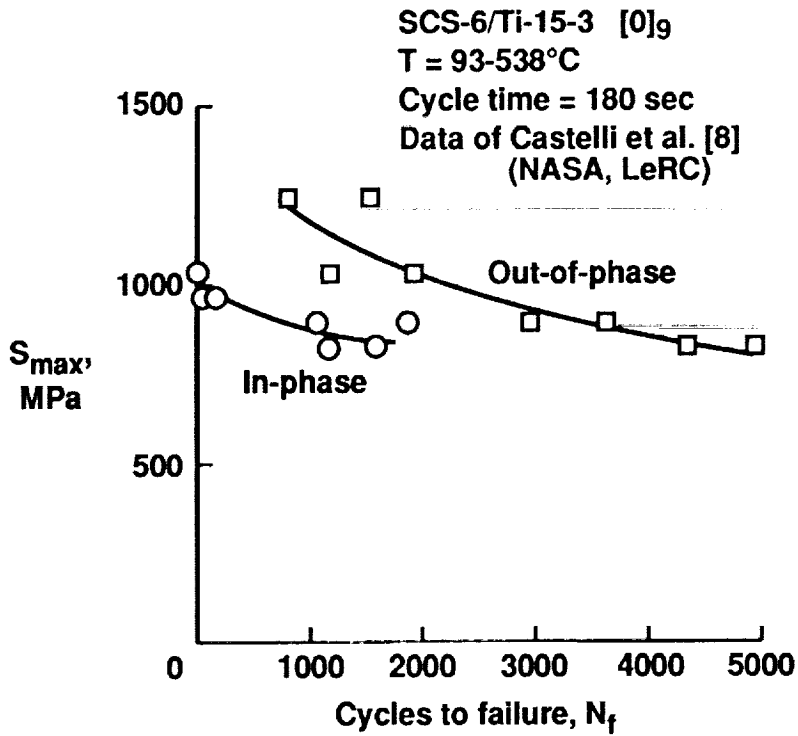
Figure 9. The maximum applied stress as a function of cycles to failure under TMF [6].
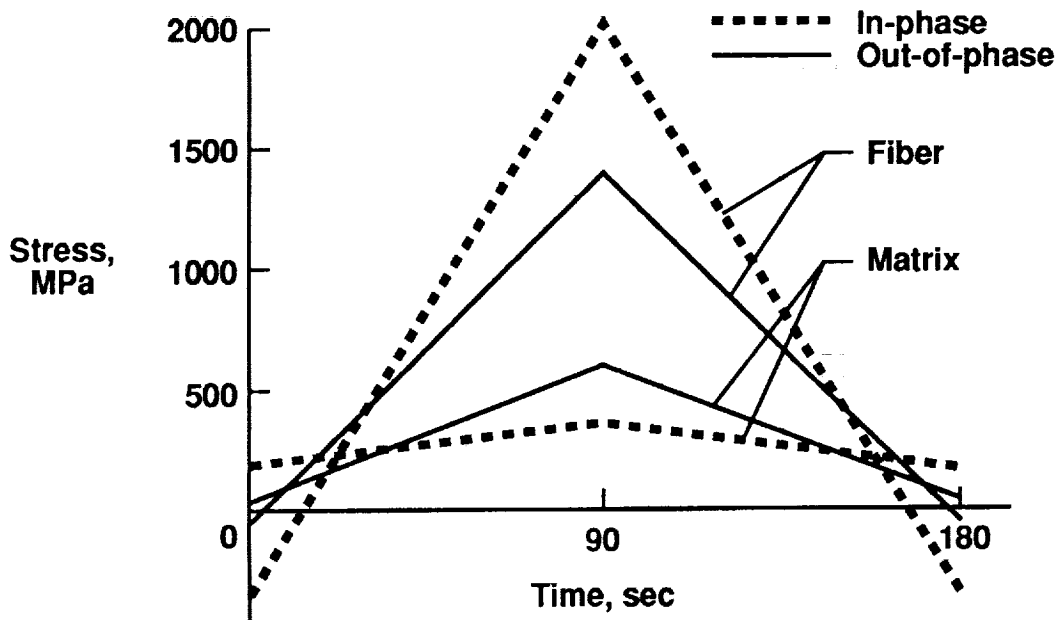
Figure 10. VISCOPLY analysis of in-phase and out-of-phase TMF [6].
Applied temperature cycled between 93 and 538°C.
Applied stress cycled between 45 and 896 MPa.

18
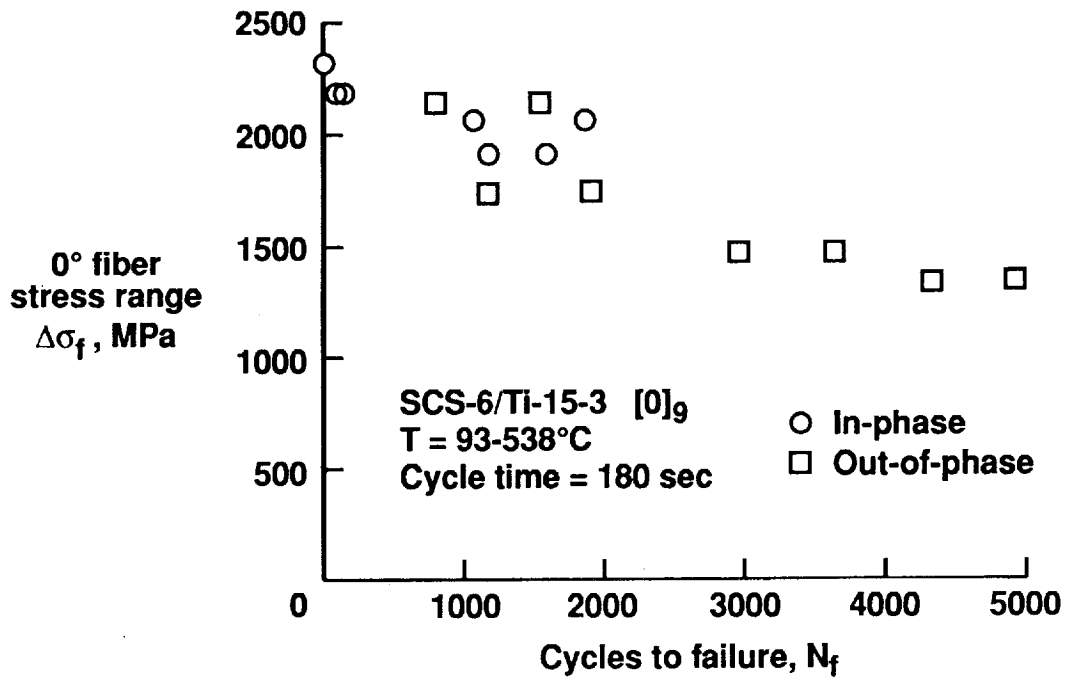
Figure 11. The stress range in the 0° fiber as a function of cycles to failure [6].
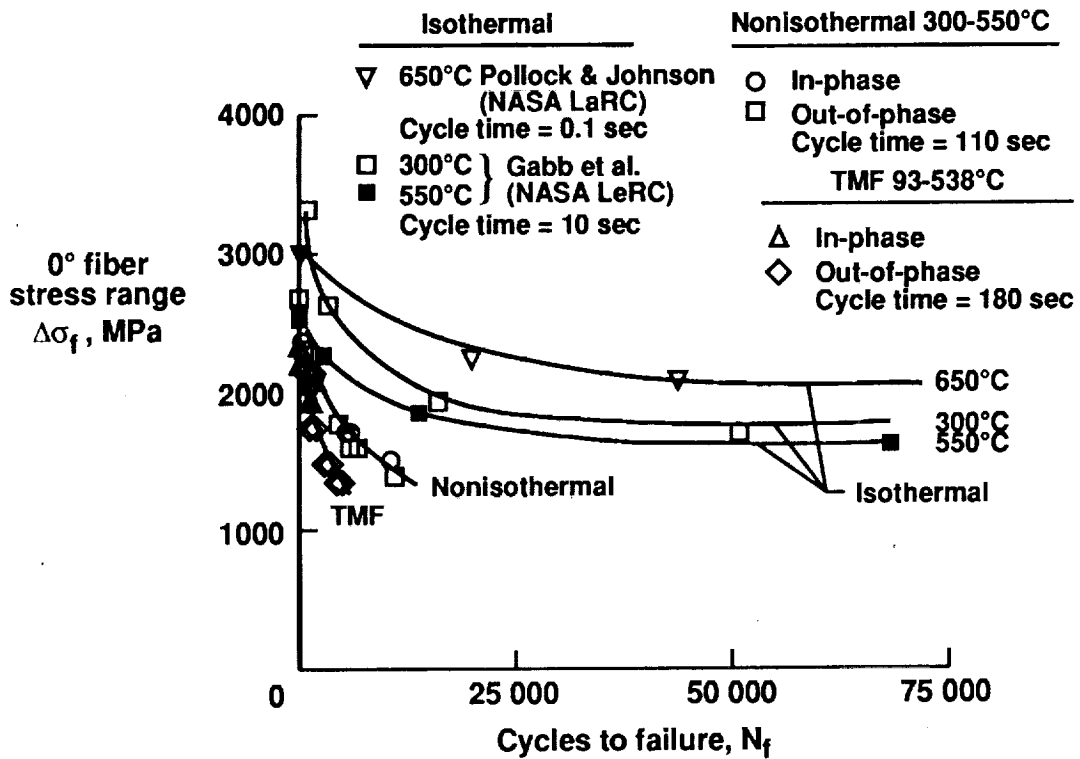
Figure 12. The stress range in the 0° fiber as a function of cycles to failure [6].

19
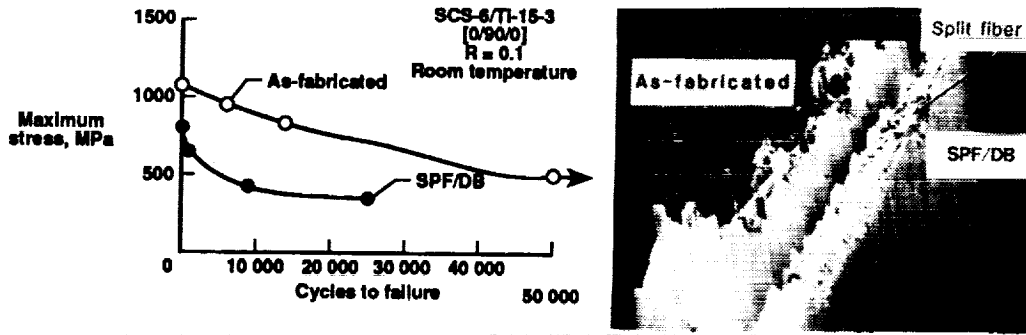
Figure 13. S-N curve for the laminates and their failure surface [10].
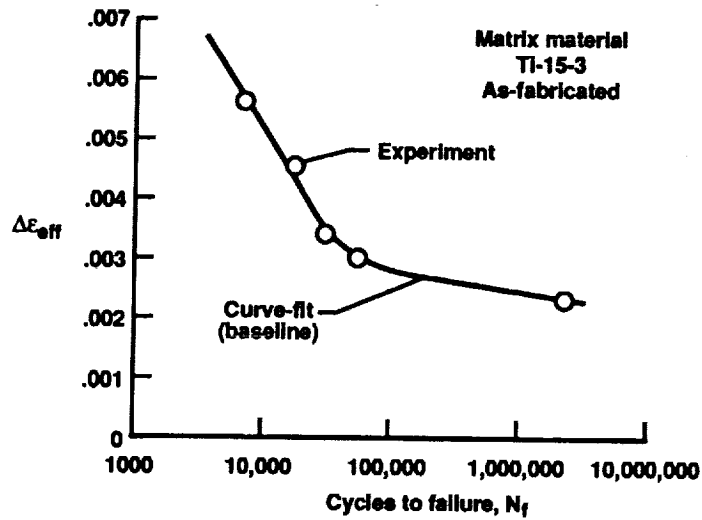
Figure 14. Strain controlled matrix fatigue data plotted in terms of effective strain criterion [12].
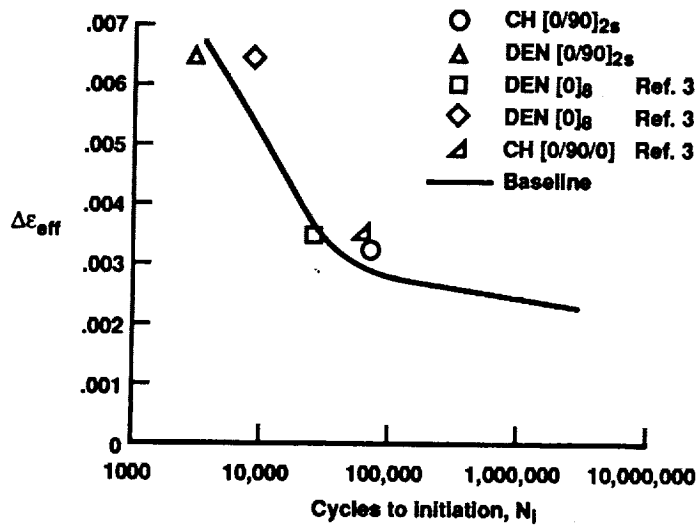

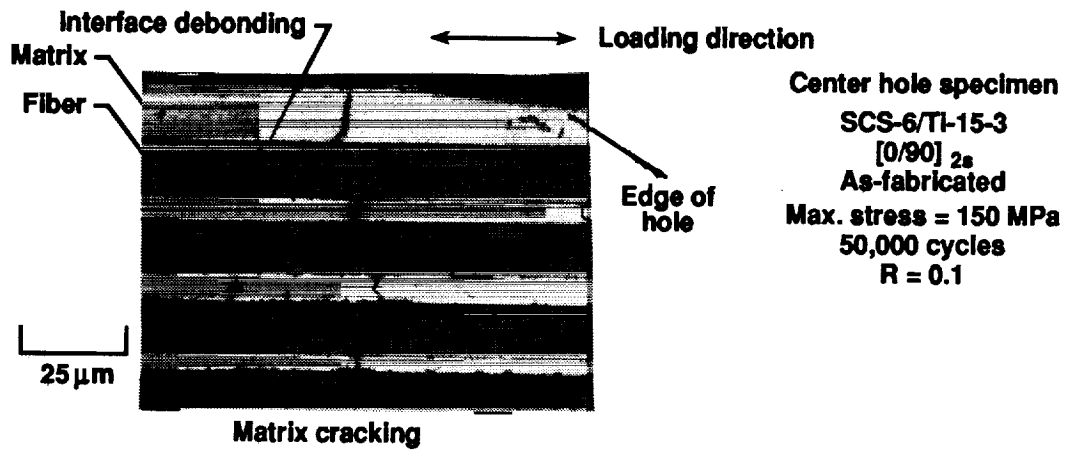Figure 15. Predicted versus experimental crack inititation [12].

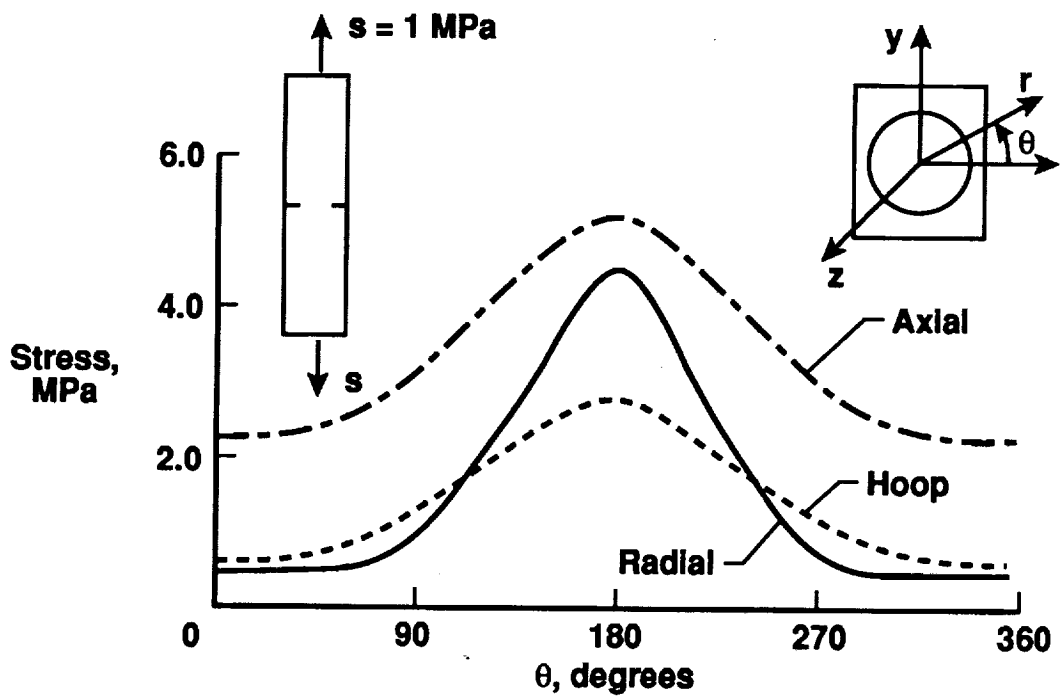Figure 16. Matrix crack growing past fibers [11].

Figure 17. Matrix stresses at fiber-matrix interface in 0° ply next to notch for
[0/90]$_{2s}$ double edge notch specimen due to unit applied stress
(S = 1 MPa). v_f = 39%, SCS-6/Ti-15-3. θ = 180° is the side of the
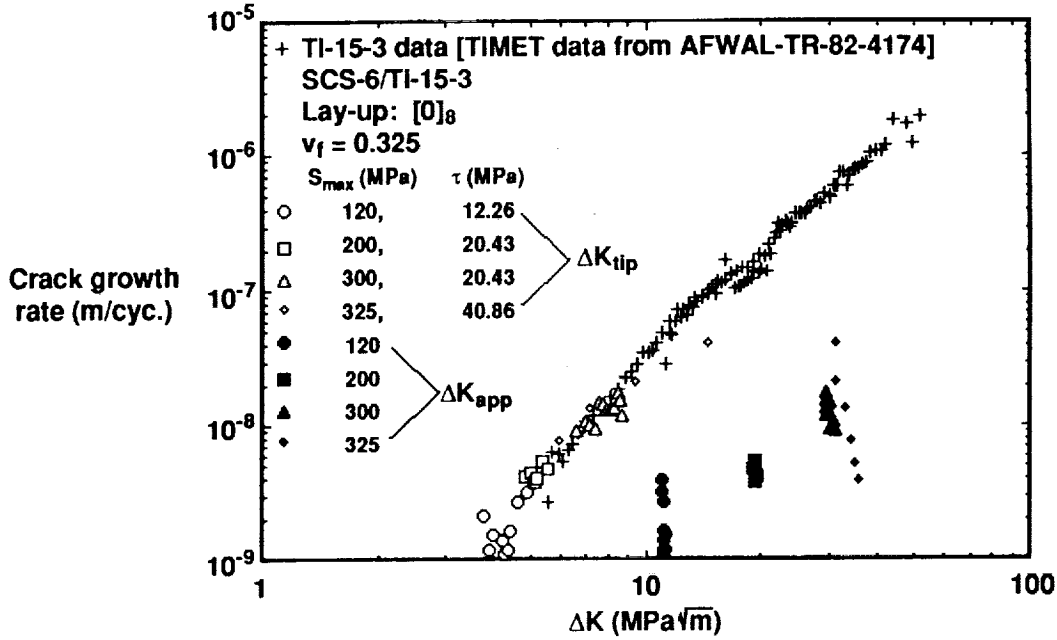fiber toward the notch tip [16].

Figure 18. Crack growth rate data from the Ti-15-3 material compared with the crack growth data from the composite. The solid symbols are the composite crack growth data assuming no fiber bridging. The open symbol data are corrected for bridging, assuming the indicated shear stresses [17].
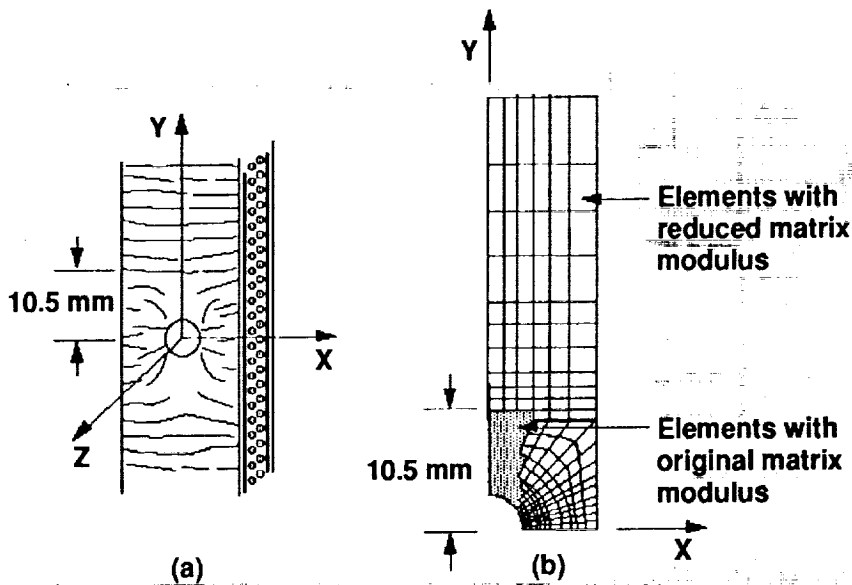

Figure 19. Specimen configuration and finite element representation for the [0/90]s SCS-6/Ti-15-3 fatigue damaged center hole specimen, $v_f = 0.355$; (a) damaged specimen showing matrix crack pattern; (b) finite element mesh with reduced matrix modulus in cracked regions and original matrix properties in uncracked regions[21].
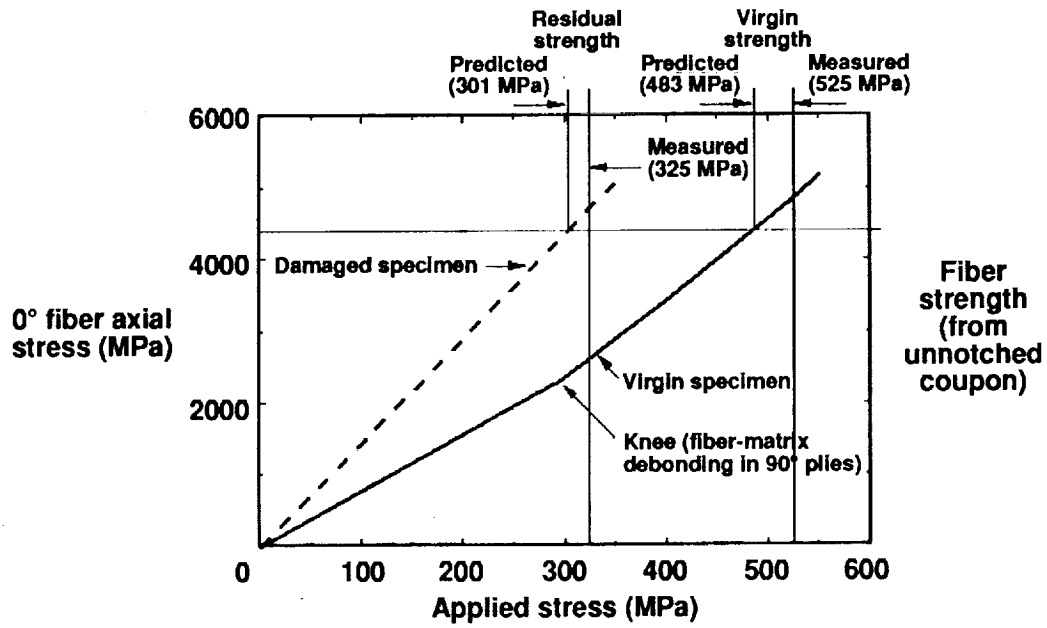
Figure 20. Axial stress in 0° fiber next to the hole as a function of applied stress for the virgin and post-fatigue conditions in[0/90]$_s$ SCS-6/Ti-15-3 laminate, v$_f$ = 0.355. Applied stress at which the 0° fiber stress reaches the fiber strength corresponds to the notched strength for both conditions [21].

REPORT DOCUMENTATION PAGE

Public reporting burden for this collection of information is estimated to average 1 hour per response, including the time for reviewing instructions, searching existing data sources, gathering and maintaining the data needed, and completing and reviewing the collection of information. Send comments regarding this burden estimate or any other aspect of this collection of information, including suggestions for reducing this burden, to Washington Headquarters Services, Directorate for Information Operations and Reports, 1215 Jefferson Davis Highway, Suite 1204, Arlington, VA 22202-4302, and to the Office of Management and Budget, Paperwork Reduction Project (0704-0188), Washington, DC 20503.

1. AGENCY USE ONLY (Leave blank)	2. REPORT DATE	3. REPORT TYPE AND DATES COVERED
	April 1992	Technical Memorandum

4. TITLE AND SUBTITLE	5. FUNDING NUMBERS
Damage Development in Titanium Metal Matrix Composites Subjected to Cyclic Loading	WU 506-43-71-01

6. AUTHOR(S)

W. S. Johnson

7. PERFORMING ORGANIZATION NAME(S) AND ADDRESS(ES)	8. PERFORMING ORGANIZATION REPORT NUMBER
NASA Langley Research Center Hampton, VA 23665-5225	

9. SPONSORING/MONITORING AGENCY NAME(S) AND ADDRESS(ES)	10. SPONSORING/MONITORING AGENCY REPORT NUMBER
National Aeronautics and Space Administration Washington, DC 20546-0001	NASA TM-107597

11. SUPPLEMENTARY NOTES

Presented as a Keynote Lecture at Fatigue and Fracture of Inorganic Composites, March 31-April 2, 1992, Cambridge, UK.

12a. DISTRIBUTION/AVAILABILITY STATEMENT	12b. DISTRIBUTION CODE
Unclassified - Unlimited Subject Category 24	

13. ABSTRACT (Maximum 200 words)

Several layups of SCS-6/Ti-15-3 composites were investigated. Fatigue tests were conducted and analyzed for both notched and unnotched specimens at room and elevated temperatures. Thermo-mechanical fatigue results were also analyzed. Tests results indicated that the stress in the 0° fibers is the controlling factor in fatigue life. The static and fatigue strength of these materials is shown to be strongly dependent on the level of residual stresses and the fiber/matrix interfacial strength. Fatigue tests of notched specimens showed that cracks can initiate and grow many fiber spacings in the matrix material without breaking fibers. Fiber bridging models were applied to characterize the crack growth behavior. The matrix cracks are shown to significantly reduce the residual strength of notched composite. The notched strength of these composites was accurately predicted using a micromechanics-based methodology.

14. SUBJECT TERMS			15. NUMBER OF PAGES
Interfaces; Stiffness loss; Finite-element analysis; Residual strength; Effective strain; Crack propagation			24
			16. PRICE CODE
			A03

17. SECURITY CLASSIFICATION OF REPORT	18. SECURITY CLASSIFICATION OF THIS PAGE	19. SECURITY CLASSIFICATION OF ABSTRACT	20. LIMITATION OF ABSTRACT
Unclassified	Unclassified		